Article

Carbon Dioxide Hydrogenation on Ni(110)

Erik Vesselli, Loredana De Rogatis, Xunlei Ding, Alessandro Baraldi, Letizia Savio, Luca Vattuone, Mario Rocca, Paolo Fornasiero, Maria Peressi, Alfonso Baldereschi, Renzo Rosei, and Giovanni Comelli

J. Am. Chem. Soc., **2008**, 130 (34), 11417-11422 • DOI: 10.1021/ja802554g • Publication Date (Web): 30 July 2008

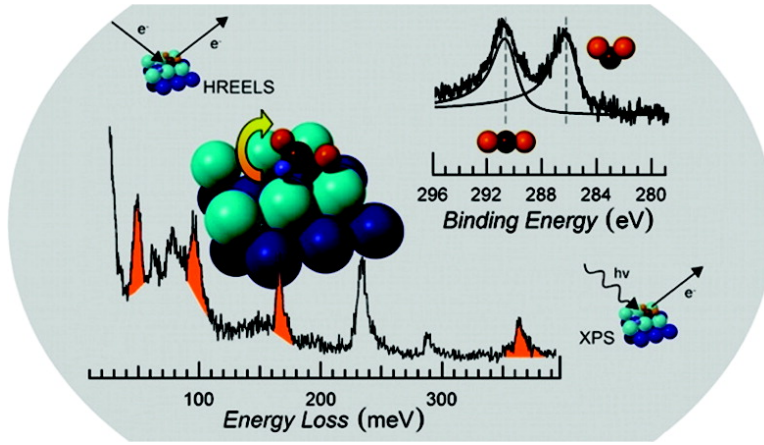

More About This Article

Additional resources and features associated with this article are available within the HTML version:

- Supporting Information
- Access to high resolution figures
- Links to articles and content related to this article
- Copyright permission to reproduce figures and/or text from this article

View the Full Text HTML

J|A|C|S
ARTICLES

Published on Web 07/30/2008

Carbon Dioxide Hydrogenation on Ni(110)

Erik Vesselli,*,† Loredana De Rogatis,‡ Xunlei Ding,§ Alessandro Baraldi,† Letizia Savio,|| Luca Vattuone,⊥ Mario Rocca,# Paolo Fornasiero,▽ Maria Peressi,○ Alfonso Baldereschi,◆ Renzo Rosei,† and Giovanni Comelli†

Physics Department and Center of Excellence for Nanostructured Materials (CENMAT), University of Trieste, Via A. Valerio 2, I-34127, Trieste, Italy, Laboratorio Nazionale CNR TASC-INFM, Area Science Park, SS 14 km 163.5, I-34012, Basovizza (TS), Italy, Chemistry Department, University of Trieste, Via L. Giorgieri 1, I-34127, Trieste, Italy; Italian Consortium on Materials Science and Technology (INSTM), Department of Theoretical Physics, University of Trieste, Strada Costiera 11, I-34014, Trieste, Italy, Theory@Elettra Group, CNR-INFM DEMOCRITOS National Simulation Center, Trieste, Italy, Institute of Theoretical Physics, École Polytechnique Fédérale de Lausanne (EPFL), CH-1015, Lausanne, Switzerland, and Physics Department, University of Genova, CNISM, Unità di Genova and IMEM-CNR, Sezione di Genova, via Dodecanneso 33, I-16146, Genova, Italy

Received April 8, 2008; E-mail: vesselli@tasc.infm.it

Abstract: We demonstrate that the key step for the reaction of CO_2 with hydrogen on Ni(110) is a change of the activated molecule coordination to the metal surface. At 90 K, CO_2 is negatively charged and chemically bonded via the carbon atom. When the temperature is increased and H approaches, the $H-CO_2$ complex flips and binds to the surface through the two oxygen atoms, while H binds to the carbon atom, thus yielding formate. We provide the atomic-level description of this process by means of conventional ultrahigh vacuum surface science techniques combined with density functional theory calculations and corroborated by high pressure reactivity tests. Knowledge about the details of the mechanisms involved in this reaction can yield a deeper comprehension of heterogeneous catalytic organic synthesis processes involving carbon dioxide as a reactant. We show why on Ni the CO_2 hydrogenation barrier is remarkably smaller than that on the common Cu metal-based catalyst. Our results provide a possible interpretation of the observed high catalytic activity of NiCu alloys.

Introduction

Carbon dioxide chemistry is of great technological interest.[1,2] Its recovery for subsequent catalytic transformation, besides limiting greenhouse effects, is a key process for the organic synthesis of chemicals like methanol (MeOH), a promising candidate as an energy carrier to feed internal combustion engines or fuel cells.[3,4] Its synthesis is generally performed on $Cu/ZnO-Al_2O_3$ based catalysts fed with a CO_2, H_2, and CO stream.[5] Interestingly, on a Ni/Cu(100) model catalyst, it was observed that (i) the turnover frequency for CO_2 hydrogenation is 60 times higher at Ni sites than at Cu sites; (ii) CO_2 is the source of carbon and oxygen; and (iii) CO is essential for promoting Ni segregation to the surface.[6−9] Formate was identified as the first intermediate of the MeOH synthesis reaction on Cu,[10−15] Ni,[16] and most transition metal surfaces or oxide-supported transition metals.[10−15,17] However, the atomic-scale details of the hydrogenation process of activated CO_2 have not yet been unraveled.

† Physics Dept., CENMAT University, of Trieste and CNR TASC-INFM.
‡ Chemistry Dept., CENMAT University, of Trieste and CNR TASC-INFM.
§ Theory@Elettra Group, CNR-INFM DEMOCRITOS, presently at Beijing National Laboratory for Molecular Sciences (BNLMS), Institute of Chemistry, Chinese Academy of Sciences, Beijing.
|| Physics Dept., University of Genova.
⊥ Physics Dept., University of Genova and CNISM
Physics Dept., University of Genova and IMEM-CNR
▽ Chemistry Dept., University of Trieste and INSTM
○ Dept. of Theoretical Physics, University of Trieste and CNR-INFM DEMOCRITOS
◆ Dept. of Theoretical Physics, University of Trieste and CNR-INFM DEMOCRITOS and EPFL

(1) Lackner, K. S. *Science* **2003**, *300*, 1677.
(2) Song, C. *Catal. Today* **2006**, *115*, 2.
(3) Sakakura, T.; Choi, J. C.; Yasuda, H. *Chem. Rev.* **2007**, *107*, 2365.
(4) Krylov, O. V.; Memedov, A. *Russ. Chem. Rev.* **1995**, *64*, 877.
(5) Hansen J. B. *Handbook of Heterogeneous Catalysis, Vol. 4*; Ertl G., Knötzinger H., Weitkamp, J., Eds.; VCH: 1997; p 1856.
(6) Rasmussen, P. B.; Kazuta, M.; Chorkendorff, I. *Surf. Sci.* **1994**, *318*, 267.
(7) Nerlov, J.; Chorkendorff, I. *Catal. Lett.* **1998**, *54*, 171.
(8) Nerlov, J.; Chorkendorff, I. *J. Catal.* **1999**, *181*, 271.
(9) Nerlov, J.; Sckerl, S.; Wambach, J.; Chorkendorff, I. *Appl. Catal., A* **2000**, *191*, 97.
(10) Hu, Z. M.; Takahashi, K.; Nakatsuji, H. *Surf. Sci.* **1999**, *442*, 90.
(11) Wang, G.; Morikawa, Y.; Matsumoto, T.; Nakamura, J. *J. Phys. Chem. B* **2006**, *110*, 9.
(12) Collins, S. E.; Baltanàs, M. A.; Bonivardi, A. L. *J. Catal.* **2004**, *226*, 410.
(13) Fujitani, T.; Nakamura, I.; Uchijima, T.; Nakamura, J. *Surf. Sci.* **1997**, *383*, 285.
(14) Jung, K. D.; Bell, A. T. *J. Catal.* **2000**, *193*, 207.
(15) Hu, Z. M.; Nakatsuji, H. *Chem. Phys. Lett.* **1999**, *313*, 14.
(16) Wambach, J.; Illing, G.; Freund, H.-J. *Chem. Phys. Lett.* **1991**, *184*, 239.
(17) Le Peltier, F.; Chaumette, P.; Saussey, J.; Bettahar, M. M.; Lavalley, J. C. *J. Mol. Catal. A: Chem.* **1998**, *132*, 91.

Very recently,[18] CO_2 hydrogenation on Cu(111) was investigated as a possible step involved in the water gas shift reaction, using Density Functional Theory (DFT) calculations. It was found that the linear CO_2 binds to Cu with a bond energy of only 0.09 eV and that the first hydrogen addition barrier (to yield formate) is 1.02 eV. Also on Pt(111),[19] CO_2 is only weakly bound (0.11 eV) to the surface, thus maintaining its linear gas phase configuration, and a barrier of 1.39 eV was calculated for the same hydrogenation step. Experimentally, on the other side, the investigation of CO_2 chemistry under UHV is not trivial, due to the extremely weak binding of the molecule to metal surfaces (generally, as in the cases of Cu and Pt, some tens of meV).

Ni(110) is the only transition metal low Miller index surface to which CO_2 chemically binds under Ultra High Vacuum (UHV) conditions without requiring coadsorption of alkali metals as electron donors.[20−22] Our previous investigations yield a CO_2 binding energy of 0.32 eV for chemisorption on Ni(110) in the hollow site with the molecular plane inclined with respect to the surface and mainly a carbon coordination with Ni (hereafter indicated as hollow-up (HU) configuration), while the linear physisorbed state is bound by only a few tens of meV, in analogy to the Cu(111) surface.[21,22] The present experimental and theoretical study provides a thorough description of the very initial steps of hydrogen reaction with CO_2 chemisorbed on Ni(110). We demonstrate that HCOO forms via a Langmuir−Hinshelwood mechanism, in line with previously reported data,[16,20] and we unravel the atomic-scale details of the reaction. Ni(110) activates the CO_2 molecule for hydrogen addition, yielding a relatively low reaction barrier (0.43 eV), compatible with high pressure observations of Ni, and NiCu alloy behavior.[6−9]

Methods

Experimental. Reactivity, electronic, and vibrational data about the CO_2 + H reaction were obtained by Temperature Programmed Desorption (TPD) spectroscopy, X-Ray Photoelectron Spectroscopy (XPS), and High Resolution Electron Energy Loss Spectroscopy (HREELS) measurements, respectively.

Experiments were carried out in two different UHV chambers. XPS and TPD analyses were performed in a multipurpose apparatus with a base pressure of 5×10^{-11} mbar equipped with Low Energy Electron Diffraction (LEED) and Spot Profile Analysis (SPA)-LEED optics, residual gas analyzer for TPD measurements, a conventional Mg Kα X-ray source ($h\nu = 1253.6$ eV, $\Delta E = 0.9$ eV), a monochromatic Al Kα source ($h\nu = 1486.6$ eV, $\Delta E = 0.4$ eV), and a VG MKII hemispheric electron energy analyzer. The sample was mounted on a 4 degrees of freedom manipulator, resistively heated, and cooled down to 90 K by liquid nitrogen flow. XPS spectra were collected at normal emission, with a source-detector angle of 55° and a pass energy of 20 eV. HREELS experiments were carried out in a dedicated chamber (base pressure of 1.5×10^{-10} mbar) with an HREELS spectrometer (SPECS), additionally equipped with a commercial LEED optics (OCI), and an XPS facility (ESCA Omicron). Here, the sample was heated by electron bombardment and/or irradiation from a hot tungsten filament, while cooling was performed by liquid nitrogen.

The Ni(110) surface was cleaned by several cycles of ion bombardment and subsequent progressive annealing up to 1300 K. Oxidation cycles were performed periodically to remove carbon contamination. Surface order and cleanliness were checked by LEED and XPS, respectively.

Core level spectra were fitted after normalization and background subtraction. For C 1*s*, a linear background was assumed, while a profile obtained from the measurement of the clean surface was used in the case of the O 1*s* spectra, due to the presence of the Ni $L_3M_{23}M_{23}$ Auger transition. The distinct contributions to the C 1*s* intensities were deconvoluted by means of a Doniach−Šunjić function,[23] convoluted with a Gaussian envelope.

HREEL spectra were recorded in specular geometry, with a primary electron energy of 3.0 eV and an incidence angle of 62°. In order to maximize the signal from the low reflectivity, disordered CO_2 + H layers, the instrument was operated at a resolution of ∼5 meV. The angular acceptance of the electron energy analyzer was 4° full width at half-maximum. HREEL spectra were normalized to the elastic peak intensity.

Theoretical Calculations. Geometries, adsorption energies, and vibrational frequencies of adsorbed HCOO as well as reaction energy barriers were calculated with the PWSCF code of the Quantum ESPRESSO distribution[24] based on spin polarized Density Functional Theory (DFT).[25] In particular, we used the generalized gradient approximation (GGA) for the exchange and correlation (XC) term in the Perdew−Burke−Ernzerhof implementation. Ultrasoft pseudopotentials from the publicly available repository of the QUANTUM ESPRESSO distribution were used (see ref 24[24] for details). The valence electronic wave functions were expanded by a plane wave basis set with a kinetic energy cutoff of 24 Ry. The Brillouin zone integration was carried out with smearing techniques using a $8 \times 8 \times 8$ k-point mesh for bulk Ni, corresponding meshes for slab supercells, and an energy broadening of 0.01 Ry. Surfaces were described as extended systems using periodically repeated supercells in a slab geometry with a (3×2) in-plane periodicity. The reported results were obtained with a Ni slab thickness of five layers and a vacuum space of 15 Å. Tests performed on nine-layer slabs and for increasing vacuum space indicated that the absolute adsorption energies in the five-layer supercell have a numerical error of ∼0.1 eV mainly due to size effects, while relative energy differences between nonequivalent configurations are already converged within 0.02 eV.

Adsorption configurations and reaction/diffusion barriers were obtained using the total-energy and force minimization method and the Nudged-Elastic-Band approach,[27] respectively.

Results and Discussion

We first performed a high pressure Temperature Programmed Reaction (TPR) experiment using unsupported metallic Ni powder as a model catalyst under a CO_2 (10%), H_2 (60%), Ar (30%) stream at 1 bar (gas hourly space velocity 6000 mL g^{-1} h^{-1}) in a quartz reactor. Reaction products were detected with a residual gas analyzer and a gas chromatograph. As expected,[3,4] carbon monoxide, methane, and water are produced (Figure 1). We remark that a constant CO_2 signal is detected in the outlet

(18) Gokhale, A. A.; Dumesic, J. A.; Mavrikakis, M. *J. Am. Chem. Soc.* **2008**, *130*, 1402.
(19) Grabow, L. C.; Gokhale, A. A.; Evans, S. T.; Dumesic, J. A.; Mavrikakis, M. *J. Phys. Chem.* **2008**, *112*, 4608.
(20) Freund, H.-J.; Roberts, M. W. *Surf. Sci, Rep.* **1996**, *25*, 225.
(21) Ding, X.; De. Rogatis, L.; Vesselli, E.; Baraldi, A.; Comelli, G.; Rosei, R.; Savio, L.; Vattuone, L.; Rocca, M.; Fornasiero, P.; Ancilotto, F.; Baldereschi, A.; Peressi, M. *Phys. Rev. B* **2007**, *76*, 195425.
(22) Ding, X.; Pagan, V.; Peressi, M.; Ancilotto, F. *Mater. Sci. Eng., C* **2007**, *27*, 1355.
(23) Doniach, S.; Šunjić, M. *J. Phys. C: Solid State Phys.* **1970**, *3*, 185.
(24) http://www.pwscf.organd http://www.quantum-espresso.org; ultrasoft pseudopotentials from the publicly available Quantum ESPRESSO table are used: Ni.pbe-nd-rrkjus.UPF, O.pbe-rrkjus.UPF, C.pbe-rrkjus.UPF, and H.pbe-rrkjus.UPF.
(25) Jones, R. O.; Gunnarson, O. *Rev. Mod. Phys.* **1989**, *61*, 689.
(26) Perdew, J. P.; Burke, K.; Ernzerhof, M. *Phys. Rev. Lett.* **1996**, *77*, 3865.
(27) Jónsson H.; Mills G.; Jacobsen K. W. Nudged Elastic Band Method for Finding Minimum Energy Paths of Transitions. In *Classical and Quantum Dynamics in Condensed Phase Simulations*; Berne, B. J., Ciccotti, G., Coker, D. F.,. Eds.; World Scientific: 1998

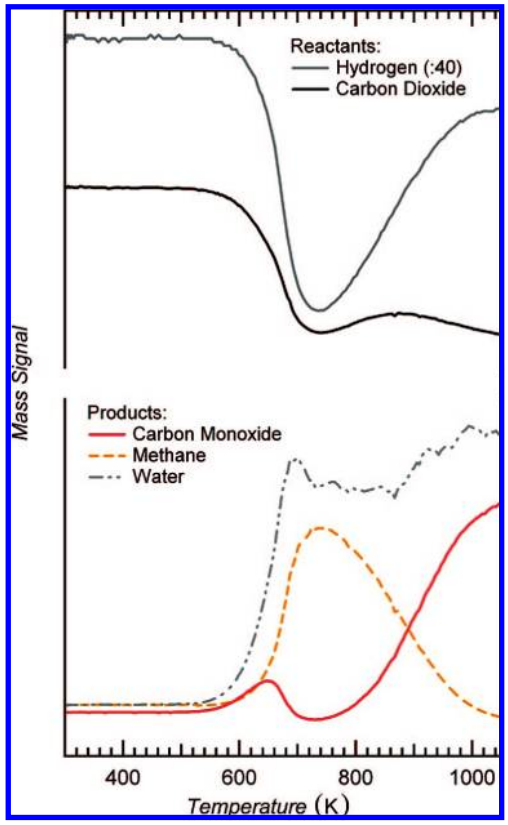

Figure 1. Results of TPR experiments performed on pure metallic Ni powder at 1 bar. An Ar-diluted CO_2 and H_2 mixture was introduced into the reactor. Heating rate is 20 K min^{-1}. Catalyst: 0.5 g of Ni; surface area: 2 m^2; avg particle size: 60 nm.

(data not shown) unless hydrogen is added to the stream, thus indicating a hydrogen-assisted CO_2 activation.

In a previous UHV study, we found that at 90 K CO_2 adsorbs molecularly on Ni(110) in both physisorbed and chemisorbed states.[21] The former readily desorbs upon heating with a main desorption peak centered at 100 K; the latter has a TPD maximum at 220 K, where desorption and decomposition into adsorbed CO and O compete against each other (Figure 2, central panel). Here we show that, upon coadsorption with hydrogen at 90 K (Figure 2, bottom panel), a new feature appears in the CO_2 TPD spectra at 305 K at the expense of the 220 K state, suggesting the formation of a reaction intermediate. Only H_2, CO, and CO_2 are detected as desorption products (0.50, 0.15, and 0.15 monolayer, respectively), upon initial exposures of 4 *L* CO_2 + 10 *L* H_2 at 90 K (1 *L* = 10^{-6} torr·s). In Figure 2, top panel, the hydrogen TPD spectrum obtained after 10 *L* H_2 at 90 K is shown for reference.

XPS spectra (Figure 3a) of the C and O 1*s* core levels were collected by stepwise annealing of both the CO_2 and the CO_2 + H layers. In the C1*s* region, CO_2 features are present at 290.6 and 286.2 eV for the physisorbed and the chemisorbed states, respectively. The carbon monoxide peak at 285.1 eV appears after annealing at $T > 220$ K.[21] For the CO_2 + H layer, an additional component is present at 288.0 eV for annealing temperatures between 150 and 300 K. We assign it to formate, based on the results of previous studies.[20,28,29] This additional

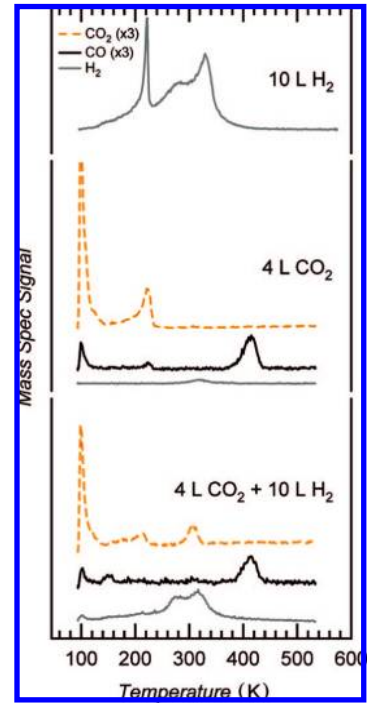

Figure 2. TPD data obtained upon exposure at 90 K of clean Ni(110) in UHV to 10 *L* H_2 (upper panel), 4 *L* CO_2 (middle panel), and to 4 *L* CO_2 + 10 H_2 (lower panel). Heating rate is 1.5 K s^{1-}.

XPS component proves that the CO_2 feature observed in the TPD spectra at 305 K is due to a dehydrogenation process of the intermediate species formed during the reaction. The intensities of the XPS components indicate that 40% of the CO_2 is hydrogenated. In the O 1*s* region (Figure 3a, left panel), the formate peak overlaps with the CO contribution at 531.0 eV. Physi- and chemisorbed CO_2, CO, and atomic O peaks are found at 534.0, 530.6, 531.0, and 529.3 eV, respectively.

HREEL spectra (Figure 3b) were collected from layers prepared following the same procedure. They confirm and complement the XPS data. At low annealing temperature ($T <$ 150 K), the spectra of the CO_2 + H layer present all the losses related to chemisorbed CO_2 and observed in the pure layer.[21] The relevant losses (see Table 1 for vibrational mode assignments) are related to CO_2 (46, 81, 90, 141, 168, 290 meV) and CO (64, 235 meV). The shoulder at 131 meV is also associated with carbon dioxide as reported in ref 21. Upon hydrogen coadsorption at 90 K, the asymmetric stretch feature of physisorbed CO_2 (290 meV) is reduced in intensity, in agreement with the XPS data which indicate a destabilization of this species in the presence of hydrogen. The intensity decrease of the loss at 141 meV due to chemisorbed CO_2 is attributed to a modification of the dynamic dipole moment upon coadsorption of CO_2 and H. A clear fingerprint of the presence of the 0.50 monolayer of hydrogen atoms in bridge sites cannot be observed due to both the low dynamical dipole moment and the overlap of the main loss expected at 80 meV[30] with the CO_2 bending mode. The spectrum at 90 K gives no evidence of losses in the C−H stretching energy range (330−380 meV), whose presence would indicate CO_2 hydrogenation. The additional weak contribution at 198 meV is probably due to water contamination,[31]

(28) Alemozafar, A. R.; Madix, R. J. *J. Phys. Chem B* **2004**, *108*, 14374.
(29) Emundts, A.; Pirug, G.; Werner, J.; Bonzel, H. P. *Surf. Sci.* **1998**, *410*, L727.
(30) Canning, N. D. S.; Chesters, M. A. *Surf. Sci.* **1986**, *175*, L811.
(31) Hock, M.; Seip, U.; Bassignana, I.; Wagenmann, K.; Küppers, J. *Surf. Sci.* **1986**, *177*, L978.

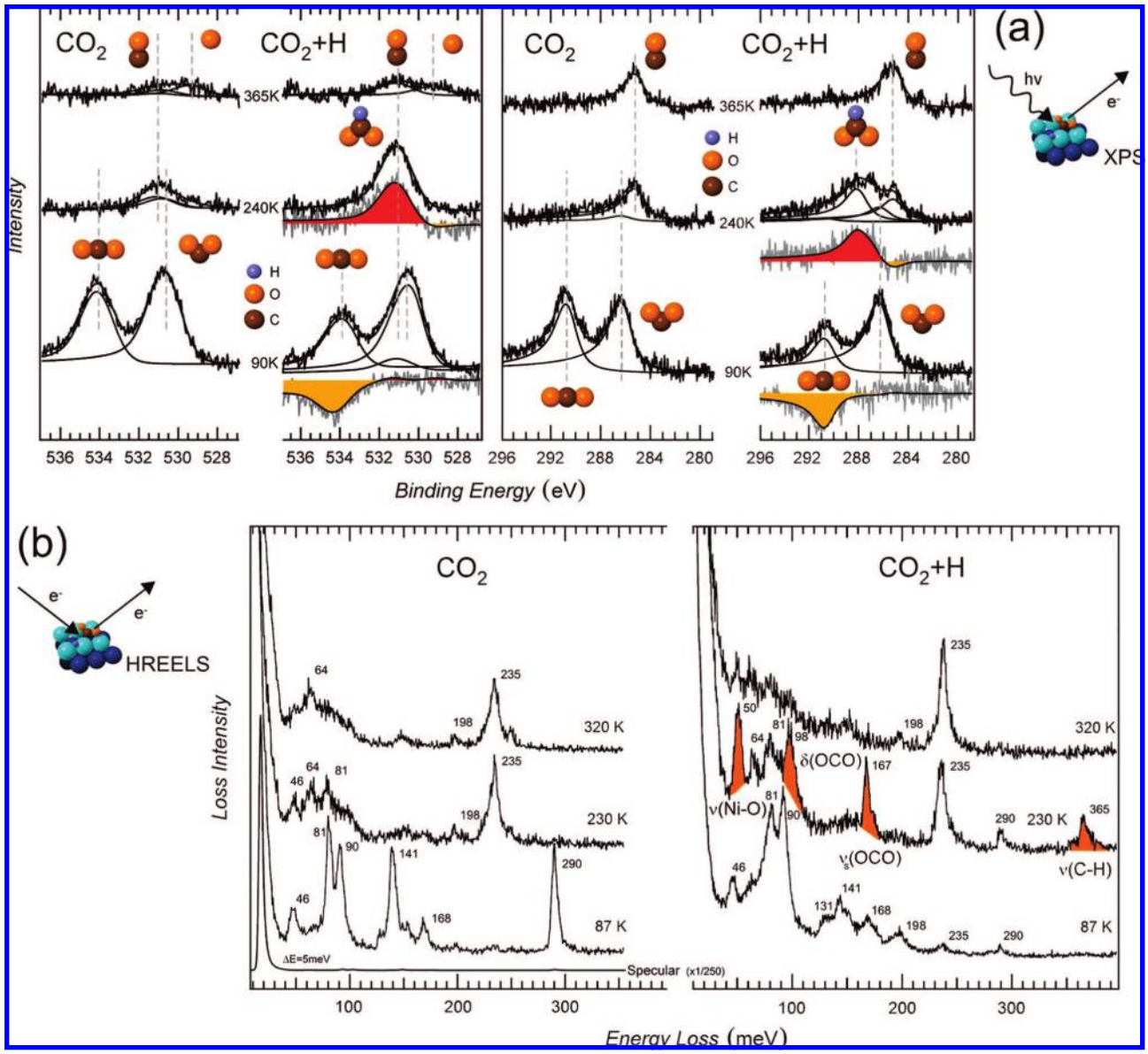

Figure 3. Spectroscopy data collected upon stepwise annealing of the CO_2 covered Ni(110) surface and of the CO_2 + H coadsorbed layer: (a) Selected XPS spectra of the O (left) and C (right) 1*s* core levels; the gray curves are difference plots between same-temperature XPS spectra of the CO_2 + H layer and of the pure CO_2 layer; additional (red) and missing (yellow) contributions are highlighted; a Mg Kα X-ray source ($h\nu$ = 1253.6 eV − ΔE =0.9 eV) was used; (b) Selected HREEL spectra of the layers prepared as in (a); the relevant HREELS losses due to HCOO (50, 98, 167, and 365 meV) are color filled. The experimental resolution was 5 meV; the primary electron energy was 3.0 eV.

detected also in the desorption spectra (<0.025 monolayer), and the one at 235 meV is due to adsorbed CO at the short bridge site.[21] In the 150−300 K temperature range, four major peaks are present at 50, 98, 167, and 365 meV. These four losses (Tables 1 and 2) are characteristic of formate adsorbed on Ni(110) in a "reversed Y" configuration.[32,33] There is no evidence of losses which could be attributed to formic acid.[20] After annealing at T > 300 K, the spectra are dominated by the carbon monoxide peak at 235 meV.

Our DFT calculations confirm that formate binds in a "reversed Y" configuration, as previously reported.[16,34] The most stable adsorption site is the short bridge (SB), which is by 0.05 eV more stable then the long bridge (LB) one (see Figure 4). The SB configuration is characterized by a C−O−C angle of 127.5° (129.8° in the LB site), which fits with a previous XPD measurement (124°).[29] The SB and LB sites are separated by a diffusion barrier of 0.55 eV (Figure 4), which is compatible with the temperature of the observed exchange process,[34] on the basis of a simple Redhead analysis.[35] According to these data, the formate measured in this work and produced by CO_2 hydrogenation should be in the SB site. However, it is not possible to confirm this conclusion on the basis of the vibrational modes, since the calculated frequencies for the two sites are very close to each other (Table 2), or considering the core level shifts (at least on the basis of a rough evaluation of the initial state contribution), since Löwdin population analysis of the

(32) Jones, T. S.; Ashton, M. R.; Richardson, N. V. *J. Chem. Phys.* **1989**, *90*, 7564.
(33) Haq, S.; Love, J. G.; Sanders, H. E.; King, D. A. *Surf. Sci.* **1995**, *325*, 230.
(34) Katano, S.; Kim, Y.; Kagata, Y.; Kawai, M. *Chem. Phys. Lett.* **2006**, *427*, 379.
(35) Redhead, P. A. *Vacuum* **1963**, *12*, 203.

Table 1. Vibrational Mode Assignment of the Losses Which Appear in the HREEL Spectra of Figure 3b

species	mode	energy (meV)
CO_2 (chem.)	Ni−CO_2	46
	bending - SB site	81
	bending - HU site	90
	symm. stretch	141
	asymm, stretch	168
CO_2 (phys.)	bending	81
	symm, stretch	168
	asymm. stretch	290
H_2O	libration	198
H	Ni−H, bridge site	131
CO	Ni−C	64
	C−O stretch, bridge site	235
HCOO	Ni−O	50
	OCO wag	98
	OCO symm. stretch	167
	C−H stretch	365

Table 2. Experimental and Calculated Vibrational Frequencies (in meV) for Formate on Ni(110)[a]

mode	exptl	theor	exptl [32,33]	exptl [32,33]
υ(NiO)	50	48 (48)	50	
δ(OCO)	98	92 (89)	95	95
υ_S(OCO)	167	160 (159)	167	168
υ(C−H)	365	365 (363)	355	352

[a] Theoretical results refer to the short-bridge adsorption geometry (long-bridge values are given in parentheses). Literature data are also quoted.

charge distribution[36,37] gives very similar results for formate in the two sites. In both cases a charge transfer of 0.62 e^- from the metal to $HCOO^{\delta-}$ occurs. With respect to the adsorbed CO_2, where the total electron transfer from the surface is 0.93 e^- (0.53 e^- on C and about 0.20 e^- on each O atom, with respect to the linear, neutral, free-standing CO_2 molecule),[21] the atomic charges on the O atoms are almost unchanged, whereas the C atom loses ∼0.25 e^-. The formate H atom becomes positively charged by 0.15 $|e^-|$, and its presence, with respect to the CO_2 molecule, reduces therefore the need for electron transfer from the metallic surface for the adsorption.

Turning to hydrogen, we found that isolated H atoms adsorb preferentially in a hollow pseudo-3-fold site (in agreement with literature data)[38−40] followed by the long bridge and the short bridge sites, characterized respectively by an adsorption energy of −2.68, −2.64, and −2.62 eV referred to an H atom in the gas phase away from the surface.

In order to study the CO_2 hydrogenation process, we consider the CO_2 molecule in the most stable HU configuration and H in an SB site as indicated in Figure 4, corresponding to the energetically favored coadsorption configuration, with a C−H distance of 2.5 Å. In this geometry, the calculated adsorption energy of the coadsorbed CO_2 and H is, within numerical accuracy, the same as the sum of CO_2 and H adsorbed separately. The structural adsorption details of the adsorbates are also unchanged, thus indicating neither mutual repulsion, nor attraction. This is not the case when H is adsorbed in pseudo-3-fold or long bridge sites close to CO_2, yielding a system energy increase up to 0.7 eV, depending on the configuration. Due to the low H diffusion barrier (0.07 eV from the pseudo-3-fold to the SB site in presence of CO_2 adsorbed in the HU configuration from our calculations, close to the 0.1 eV reported for isolated H adsorbed on the same Ni surface),[41] H hopping to the SB site can indeed easily occur. The calculated barrier for the first hydrogenation of chemisorbed CO_2 is 0.43 eV (Figure 4), in agreement with our experimental finding that the reaction occurs above 150 K (corresponding to an activation energy of 0.40 eV on the basis of the Redhead model).[35] Furthermore, the calculated barrier for C−H bond cleavage of adsorbed formate is 0.97 eV. This value is in good agreement with the activation energy of 1.06 eV measured for both dehydrogenation and dehydration of formate adsorbed on Ni(110),[42,43] thus confirming that the two decomposition processes proceed simultaneously and that C−H bond scission is their common rate-determining step.

On the basis of the above considerations, we can now provide the following full description for the mechanism. On Ni(110) at low T, CO_2 is negatively charged and is chemically bonded mainly via the carbon atom. The molecule receives electronic charge from the metal, bends, and binds to the surface with the carbon atom in a "V" configuration: the resulting energy barrier (0.43 eV) for its hydrogenation is relatively small and, most importantly, smaller than that for CO_2 desorption and that for dissociation into CO + O. Indeed, the latter competing processes were found to have an activation barrier of 0.60 eV.[21] When adsorbed H approaches CO_2, the H−CO_2 complex flips and binds to the surface with the two oxygen atoms and H binds to the carbon atom, thus yielding the formate intermediate which is known to exist in such a configuration[23] and to be present also under real catalyst working conditions.[17] The presence of hydrogen steers the reaction in the desired direction and prevents the formation of CO which, in analogy to what reported for the catalytic system at high pressure,[6−9] is unreactive. This is the key point of CO_2 + H chemistry on Ni(110), since the charge transfer from the metal to the molecule yields an activated state which is reactive with hydrogen via an induced flip of the complex. This process is quite different with respect to the case of Cu, which is conventionally adopted for the MeOH synthesis via CO_2 hydrogenation. Indeed, it has been shown very recently that on Cu(111) and Pt(111) hydrogen reacts with the linear CO_2 molecule, which is not activated due to the very weak metal−CO_2 interaction; this process requires then a much higher reaction barrier (1.02 and 1.39 eV, respectively) than the 0.43 eV we find on Ni(110). This provides possible explanations for the peculiar behavior of the CO_2 + CO + H_2 reaction on the NiCu alloy,[6−9] where a higher turnover frequency was indeed found for CO_2 conversion at Ni sites with respect to Cu sites. The role of unreactive CO, which is an essential ingredient of the feedstock, is only to promote the active Ni segregation to the catalyst's surface.

The next step of the reaction mechanism may occur again at the carbon atom due to its residual valence, thus forming an unstable dioxomethylene intermediate which undergoes sudden C−O bond decomposition. Other pathways may also be considered since, on surfaces like Cu(111) and Pt(111),[18,19] formate was detected as a stable product species as well. HCOO is however not directly involved in the favored reaction path

(36) Szabo, A.; Ostlund, N. In *Modern Quantum Chemistry*; Dover: New York, 1996; p 153.
(37) Löwdin, P. O. *J. Chem. Phys.* **1950**, *18*, 365.
(38) Nørskov, J. K. *Phys. Rev. Lett.* **1982**, *48*, 1620.
(39) Lapujoulade, J.; Neil, K. S. *Surf. Sci.* **1973**, *35*, 288.
(40) Kresse, G.; Hafner, J. *Surf. Sci.* **2000**, *459*, 287.
(41) Bhatia, B.; Sholl, D. S. *J. Chem. Phys.* **2005**, *122*, 204707.
(42) Benziger, J. B.; Madix, R. J. *Surf. Sci.* **1979**, *79*, 394.
(43) Yamakata, A.; Kubota, J.; Kondo, J. N.; Hirose, C.; Domen, K. *J. Phys. Chem. B* **1997**, *101*, 5177.

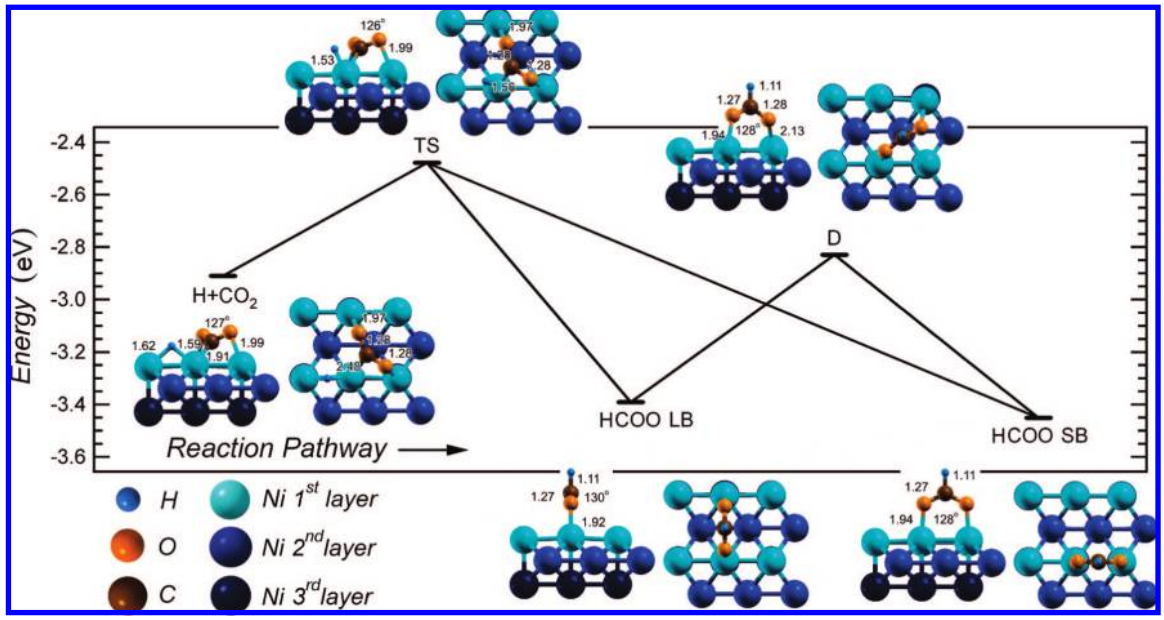

Figure 4. Results of DFT calculations for the $CO_2 + H \rightarrow HCOO$ reaction. Energies (with respect to gas-phase H and CO_2) and geometries are given for the most relevant states. LB and SB indicate the long- and short-bridge adsorption sites of HCOO, respectively; TS indicates the transition state of the reaction, and D, that of formate diffusion. Only Ni atoms of the outer layers are shown, but a five-layer thick slab has been used in the calculations.

that proceeds via carboxyl intermediates under high pressure conditions. This may contribute to a better understanding of the differences in the competing mechanisms of the reverse Water Gas Shift and MeOH synthesis reactions. HCOO formation is in addition not the rate-limiting step for CO_2 hydrogenation on Ni(110). The subsequent step is characterized by a much higher barrier since it cannot be overcome in UHV coadsorption experiments. A 10 orders of magnitude reduction of the reactant pressure at RT with respect to the standard conditions results indeed in ~0.6 eV less free energy, i.e. chemical potential,[44] per H_2 molecule available for the reaction.

Conclusions

The CO_2 molecule adsorbs on Ni(110) in a negatively charged, bent, and carbon-bonded "V" shape configuration.[20,21] By means of combined experimental and computational investigations, we have shown that H bonding to the carbon atom makes the otherwise saturated oxygen atoms of the adsorbed CO_2 molecule available for surface coordination, yielding formate, which is bound to the metal surface in a "reversed Y" configuration. Our main finding is that the reaction proceeds via a flip of a $H-CO_2$ complex which is formed upon H reaction with the activated chemisorbed CO_2 molecule. This result is at variance with earlier, currently accepted, suggestions and provides the atomic-level evidence of a lower reaction barrier on Ni with respect to the one recently reported for the same reaction on Cu.

Acknowledgment. We acknowledge financial support from MUR under programs FIRB2001 and FISR2002 "Fuel Cells", from Fondazione CRTrieste in the framework of a research grant assigned to G. Comelli, INSTM, Compagnia S. Paolo. Computational resources have been obtained within the "Iniziativa Trasversale di Calcolo Parallelo" of CNR-INFM and within the University of Trieste - CINECA agreement. We thank F. Ancilotto and F. Esch for fruitful discussions. We acknowledge technical support from Osram SpA.

JA802554G

(44) Hendriksen, B. L. M.; Bobaru, S. C.; Frenken, J. W. M. *Top. Catal.* **2005**, *36*, 43.